ISSN 2072-5981

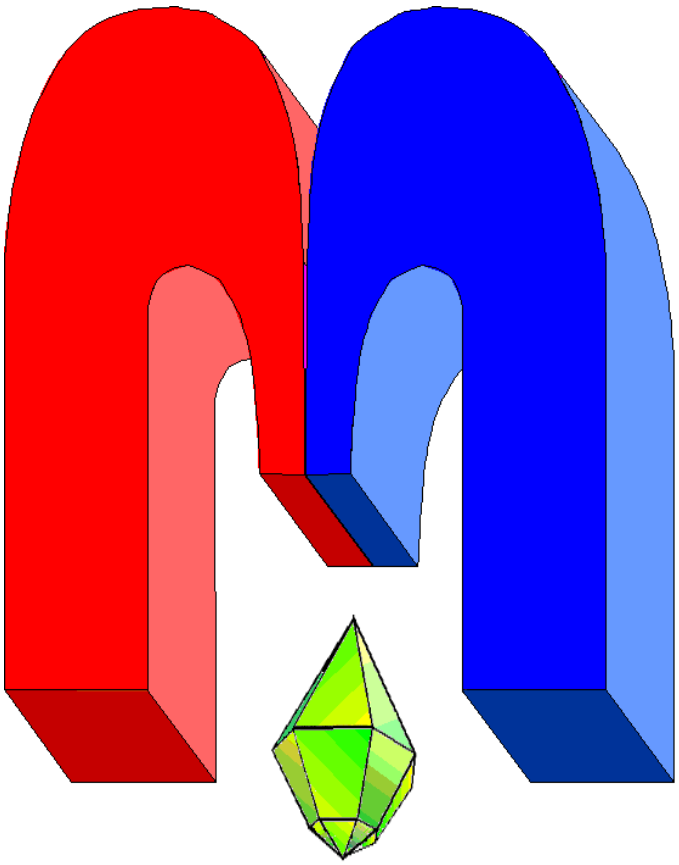

Magnetic Resonance in Solids

Electronic Journal

Volume ***18,***
Issue ***2***
Paper No ***16209,***
1-9 pages
2016

http://mrsej.kpfu.ru
http://mrsej.ksu.ru

Established and published by Kazan University
Sponsored by International Society of Magnetic Resonance (ISMAR)
Registered by Russian Federation Committee on Press, August 2, 1996
First Issue was appeared at July 25, 1997

"***Magnetic Resonance in Solids. Electronic Journal***" (**MRS*ej***) is a peer-reviewed, all electronic journal, publishing articles which meet the highest standards of scientific quality in the field of basic research of a magnetic resonance in solids and related phenomena. **MRS*ej*** is free for the authors (no page charges) as well as for the readers (no subscription fee). The language of **MRS*ej*** is English. All exchanges of information will take place via Internet. Articles are submitted in electronic form and the refereeing process uses electronic mail. All accepted articles are immediately published by being made publicly available by Internet (http://**MRS*ej***.kpfu.ru).

* In Kazan University the Electron Paramagnetic Resonance (EPR) was discovered by Zavoisky E.K. in 1944.

New vector/scalar Overhauser DNP magnetometers POS-4 for magnetic observatories and directional oil drilling support†

V.A. Sapunov [1,*], A.Y. Denisov [1], D.V. Saveliev [1], A.A. Soloviev [2,3], S.Y. Khomutov [4], P.B. Borodin [5], E.D. Narkhov [1], A.V. Sergeev [1], A.N. Shirokov [1]

[1] Ural Federal University, Quantum Magnetometry Laboratory, Mira 21, Ekaterinburg 620002, Russia

[2] Geophysical Center, RAS, Molodezhnaya 3, Moscow 119296, Russia

[3] Schmidt Institute of Physics of the Earth, RAS, B. Gruzinskaya 10, Moscow 123242, Russia

[4] Institute of Cosmophysical Research and Radio Wave Propagation, FEB RAS, Mirnaya 7, Kamchatskiy Kray, Paratunka 684034, Russia

[5] Geophysical Observatory "Arti", Institute of Geophysics, UB RAS, Geofizicheskaya 2a, Sverdlovskaya oblast, Arti 623341, Russia

E-mail: vasapunov@urfu.ru

(Received December 5, 2016; accepted December 12, 2016)

This paper covers same results of the research directed at developing an absolute vector proton magnetometer POS-4 based on the switching bias magnetic fields methods. Due to the high absolute precision and stability magnetometer POS-4 found application not only for observatories and to directional drilling support of oi and gas well. Also we discuss the some basic errors of measurements and discuss the long-term experience in the testing of magnetic observatories ART and PARATUNKA.

PACS: 75.20.-g, 76.30.Mi, 81.05.ug

Keywords: magnetometer, Overhauser dynamic nuclear polarization, nitroxide radical solution, magnetic observatory, INTERMAGNET, directional drilling

1. Introduction

The physical base of proton Overhauser magnetometry is a Larmor precession of nuclear magnetic moments in a magnetic field. Proton magnetometers determine an absolute value of the measured magnetic field induction T_0 [1]

$$T_0 \equiv \left|\mathbf{T}_0\right| = \gamma_p^{-1}\omega_0, \quad \mathbf{T} \equiv \vec{\mathrm{T}}, \tag{1}$$

where $\gamma_p = 2\pi \cdot 0.0425764$ rad/(nT·s) [2] denotes the proton gyromagnetic ratio and ω_0 is the frequency of proton precession. These magnetometers are well-known as high precision stable sensors of magnetic field absolute value. They are widely used in various applications including geophysics and observatory measurements. Fig. 1 shows the general scheme of proton precession Overhauser dynamic nuclear polarization (DNP) measurement (Overhauser magnetometer).

In addition, there were developed absolute vector proton magnetometers based on the switching of bias magnetic fields (for example [3]). In recent years, the development of proton vector magnetometers achieved significant progress due to implementation of the DNP Overhauser effect due to electron subsystem excitation.

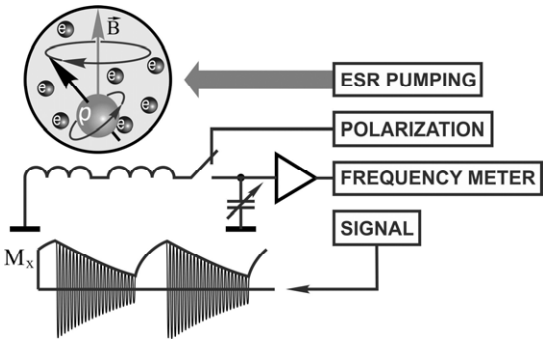

Figure 1. General scheme of DNP measurements.

† This paper material was selected at XIX International Youth Scientific School "Actual problems of magnetic resonance and its application", Kazan, 24 – 28 October 2016. The paper was recommended to publication in our journal and it is published after additional MRSej reviewing.

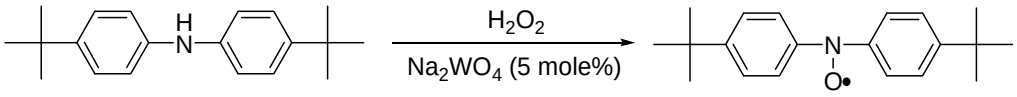

Figure 2. Synthesis and structure of a radical of the magnetometer POS-4.

We developed synthesis method of a stable radical (Fig. 2) used in our quantum magnetometers demonstrating easy electron paramagnetic resonance (EPR) saturation at medium concentrations providing high amplification DNP even for EPR superfine structure.

This radical has a record stability superior stability standard nitroxide spin labels several times. There are also benefits for hyperpolarization and ease saturation of 2 Oe of HF saturation matching half of the maximum value DNP at the general electron resonance spectrum width up to 25 Oe. For infinite polarization, the DNP signal gain coefficient is given by:

$$A_\infty = -\xi f \frac{\omega_S}{\omega_I} \frac{\varphi + kcT_{1S}}{1 + kcT_{1S}}, \tag{2}$$

where $\omega_{S,I}$ denotes electron, proton resonant frequency, $f = 1 - T_{1p}/T_{10p}$ is the loss factor, where T_{1p} is proton time relaxation of a radical solution and T_{10p} denotes proton relaxation of pure solvent. ξ is the dynamic electron-nuclear binding parameter of radical and proton in solution in the range −1 to 0.5, T_{1S} is the transversal relaxation time of electron subsystem, φ is estimated approximately as the inverse number of the saturated partial lines in the super hyperfine structure of the spectrum of electron spin resonance, k is spin exchange constant between the radicals, c is concentration of solution. At present, this effect called Heisenberg hyperpolarization is widely being studied [4]. It should be noted that the single line with the weight φ in the EPR spectrum is saturated but in DNP effect we saturate all the lines simultaneously. In addition to the hyperpolarization it leads to a decrease of the required electronic pump field. This light saturation effect is important for the Overhauser magnetometers. Additional gain provides stronger proton signal from smaller sensor size. This allows reduce dimensions of the magnetic bias systems and as consequence, to improve measurements sensitivity.

2. Method of measurement based on switched bias fields

To measure the components of the geomagnetic field by a proton (scalar) magnetometer a number of methods are known. We investigate below the setup based on the switching of bias magnetic fields **B** (cycle: $-I$, $I = 0$, $+I$) with the measurement of resulting total field. The vector diagram for a switching method (Fig. 3) and formula (3) for calculation of the field component Z along the bias field ($Z = T_0 \cdot \cos(\alpha)$) are shown below:

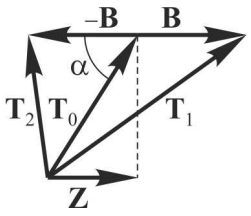

Figure 3. Vector diagram for switching method of Z component measurement.

$$Z = \frac{1}{2\sqrt{2}} \frac{T_1^2 - T_2^2}{\sqrt{T_2^2 + T_1^2 - 2T_0^2}}, \quad \mathbf{T}_{1,2} = \mathbf{T}_0 \pm \mathbf{B}. \tag{3}$$

It is a well-known formula, but, unfortunately, it does not provide any useful information to select value and direction of the bias field. Nor does it determine the effect of the selected parameters upon the resulting random and systematic measurements errors of Z.

3. Sensitivity or random error of the component measurement

Let's assume identical sensitivity for all measurements of the field absolute value $\sigma(T_0) = \sigma(T_2) = = \sigma(T_1) = \sigma(T)$. The dispersion of Z component measurement reads

$$\sigma^2(Z) = \sigma^2(T)\left[1 - \frac{1}{2}\left(1 - \frac{T_0^2}{B^2}\right)\left(1 + 3\frac{T_0^2}{B^2}\cos(\alpha)^2\right)\right]. \quad (4)$$

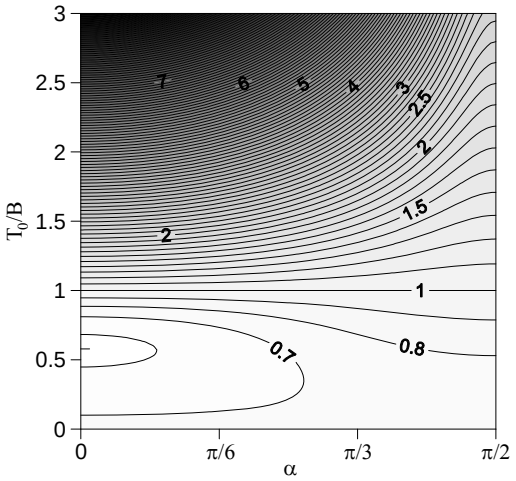

Figure 4. Loss of sensitivity of vector measurements in comparison to scalar magnetometer depending on the angle orientation of the field and their strengths ratio.

Fig. 4 shows the ratio $\sigma(Z)/\sigma(T)$ representing sensitivity deterioration sensitivity of the Z component measurements compared to sensitivity of the scalar magnetometer as a function of the ratio of the geomagnetic field modulus to value of the bias field T_0/B at various angles between them.

There is an optimum angle at "magic" angle $\alpha \le \arccos(3^{-1/2}) \approx 54°44'$. The optimum would be for the following field relationship

$$\frac{T_0}{B} = \sqrt{\frac{3\cos(\alpha)^2 - 1}{6\cos(\alpha)^2}}. \quad (5)$$

The value is minimal at $\alpha = 0$, $T_0/B = 3^{-1/2} \approx 0.58$ when the loss of sensitivity is $\sigma(Z)/\sigma(T) = 3^{-1/2}$. Unfortunately, this case is not interesting in practice because the increase of the bias field causes an increase of its gradient that means too high requirements from the bias magnetic system. Also, there is a restriction on the bias field amplitude due to the dynamic range of the proton magnetometer (usually 20000 ÷ 100000 nT). More interesting is the intermediate case, when the sensitivity of component measurements does not depend on the orientation of the bias magnetic field and total intensity. This bias field should be approximately 70% of the geomagnetic field, with a factor 1.5 ÷ 2 in the deterioration of sensitivity.

4. Some systematic errors of the component measurement

Next, we analyze the main contributions to the systematic error caused by various reasons occurring during vector measurements technique based on switched bias fields. The systematic error of the measurement is defined as follows $\Delta Z = Z - Z_0$, where Z is the measured field component (3) and Z_0 is the true component value.

4.1 Errors caused by "soft" and "hard" magnetization of the module sensors

Field modulus errors caused by the "soft" magnetisation of the magnetometer sensors (magnetic moment of the sensor is proportional to the external field) are defined as $\Delta T_1 = \eta T_1$, $\Delta T_2 = \eta T_2$, $\Delta T_0 = \eta T_0$, where $\Delta \mathbf{T}_i \equiv \mathbf{T}_i' - \mathbf{T}_i$, $\mathbf{T}_i'$ is a result of actual measurement, $\mathbf{T}_i$ is a true vector without the account of the magnetization field. Using the formula (3) it is possible to draw a simple but important conclusion:

$$\Delta Z_{\text{soft}} = \eta Z. \quad (6)$$

Thus, the error of the component measurement caused by the "soft" magnetization of its absolute magnetometer sensor is fully eliminated by the calibration of the module sensor.

The error due to the "hard" magnetization of the module sensor means that the sensor has its own magnetic moment due to some internal magnetic field **h** from a magnetic impurity. In this case the component of the field $\mathbf{T}_0' = \mathbf{T}_0 + \mathbf{h}$ will be measured. The final expression of the "hard" error will be

$$\Delta Z_{\text{hard}} = (\mathbf{h}\cdot\mathbf{B})/B = h\cdot\cos(\theta), \quad (7)$$

where θ is an angle between the bias field vectors **B** and internal field **h**.

Thus:

- The systematic error of component measurement caused by the "hard" errors of the module sensors depends only on the angle between the internal proton sensor "hard" field and the bias field. It does not depend on orientation of Earth's magnetic field.
- This error can be determined for some orientation of the vector magnetometer w.r.t. the Earth's field and then can be used as a correction at any field angles of declination and inclination. This error can be even completely eliminated for a special orientation of the proton sensors to bias field ($\cos(\theta) = 0$).

4.2 Error caused by instability of the bias field or the power source

Error caused by instability of the bias field or the power source is a technically important kind of the error since it defines the requirements to the stability of the magnetic bias system and source of the switched current.

We write the expression for the vector component in the case of the switching method with different bias fields **B** and $\beta\mathbf{B}$ (i.e. $\mathbf{T}_1 = \mathbf{T}_0 + \mathbf{B}$, $\mathbf{T}_2 = \mathbf{T}_0 + \beta\mathbf{B}$). The value Z in the switching set-up in this case is:

$$Z = \frac{T_1^2\beta^2 - T_2^2 + T_0^2(1-\beta^2)}{2\sqrt{\beta(\beta-1)\left(T_2^2 - \beta T_1^2 - (1-\beta)T_0^2\right)}}. \tag{8}$$

The considered instability is caused by the difference of the fields $+\mathbf{B}$ and $-\mathbf{B}$, that is $\beta\mathbf{B} = -\mathbf{B} + \Delta\mathbf{B} = -\mathbf{B}\cdot(1 - \Delta\beta)$. Correspondingly, in (8) the factors $\beta = \Delta\beta - 1$. Assuming $\Delta\beta << 1$, we find the error caused by the instability of the bias field or the power source as:

$$\Delta Z_{inst} = \frac{\Delta B}{2}\left(1 - \frac{T_0^2}{B^2}\cos(\alpha)^2\right) = \frac{B}{2}\frac{\Delta I}{I}\left(1 - \frac{T_0^2}{B^2}\cos(\alpha)^2\right). \tag{9}$$

Here we assume that the error is due to current instability during the measurement of component $\Delta B/B = \Delta I/I$.

Estimate the requirements on stability for the bias field or $\Delta I/I$ in conditions close to optimum (T_0/B about 1.5, B about 30000 nT) and setting error $\Delta Z \approx 1$ nT. We find the value of $\Delta I/I$ about 10^{-4}. Thus requirements to short-term stability of the current and bias field can be met engineering-wise and we have errors of $0.1 \div 1$ nT for instability $10^{-5} \div 10^{-4}$. It is important to note that the long-term stability does not exert influence on the switching method in contrast to a method of the field component compensation.

4.3 Error caused by the drift of the geomagnetic field

It was revealed at experimental research of the Overhauser vector magnetometers in laboratory conditions, which were characterized by fast changes of the geomagnetic field, that the switching method has also a dynamic error. To estimate the error caused by a field variation in the measurement cycle, the jump function model of a variation was simulated [5]. Namely: at the first measurement the geomagnetic field is displaced by $-\Delta\mathbf{h}$ ($\mathbf{T}_2' = \mathbf{T}_2 - \Delta\mathbf{h}$), in the second there is no displacement ($\mathbf{T}_0' = \mathbf{T}_0$) and in the third the field is displaced by $\Delta\mathbf{h}$ ($\mathbf{T}_1' = \mathbf{T}_0 + \Delta\mathbf{h}$). A vector magnetometer will calculate the Z field component according to the basic formula (3). The error is defined as the difference between the measured and calculated component without the drift $\Delta\mathbf{h}$ that is $\Delta Z_1 = Z' - Z$:

$$\Delta Z_{\text{drift}} = B^{-3}\left(\left[\mathbf{T}_0 \times \mathbf{B}\right]\cdot\left[\Delta\mathbf{h} \times \mathbf{B}\right]\right) \le \Delta h T_0 / B. \tag{10}$$

The analysis of this result shows that the drift error is due to a dynamic cross effect:

- There is an influence (error) at the presence of variations of perpendicular components.
- The error is proportional to speed of variation, more precisely it is proportional to field change during the measurement cycle (~ the discretized time derivative of field).

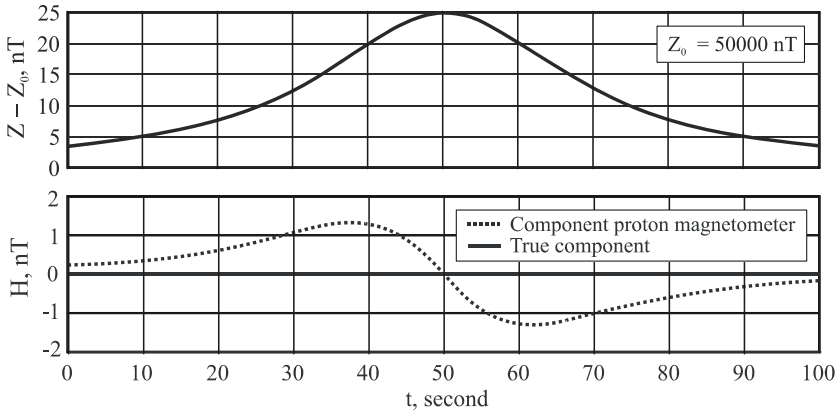

Figure 5. Error caused by the drift of the geomagnetic field as result of dynamic cross effect for the proton vector magnetometers (the cycle at calculations is 3 s).

Fig. 5 shows an example of the drift error calculation. The top panel is a simulated *Z*-variation. The bias magnetic fields **H** is perpendicular to **Z** and the measurement of *H*-component of the external field is made along **H**. The actual variation in **H** direction is absent.

Some discrepancy of variation measurements by the fluxgate and the proton vector magnetometers thus should be observed. Obviously the drift error can be excluded by some modernization of the basic formula (3) or at processing measurements taking into account speed of the components variation.

5. POS-4 design and results of testing

Due to the high absolute precision (sensitivity up to 0.01 nT and absolute scalar measurements error up to 0.1 nT at stability measurements 0.02 ÷ 0.05 nT per year) scalar Overhauser magnetometer POS-1 has wide application in the magnetic observatories and hazard monitoring systems. The Quantum Magnetometry Laboratory designed and developed the new scalar/vector magnetometer POS-4 (Fig. 6) based on the module sensor POS-1.

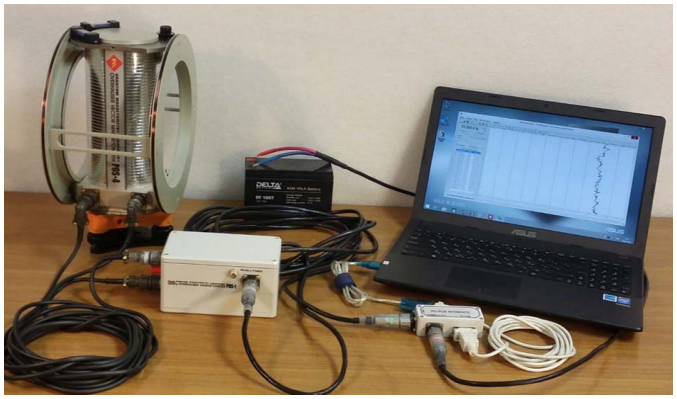

Figure 6. Vector/scalar Overhauser DNP magnetometer POS-4.

The system consists of bias coils mounted on the titanium frame. Vertical solenoid provides a measurement of the vertical *Z* component. The solenoid consists of a cylindrical titanium pipe with perpendicularly welded plates. Precision machining ensures perpendicular to both the axis of the solenoid and the plates. Two perpendicular liquid horizon levels (accuracy of 10 to 20 arc seconds) mounted on top of the plane supplemented by installing electronic levels to within 1 arc second.

Solenoid wire fits the groove geometry defined by the known Garrett solenoid conditions providing maximum uniformity of the field in the largest volume. The perpendicular Helmholtz coils or a more complex system with high uniformity of the horizontal component measurement is oriented generally for the direction north-south. The electronics unit POS-4 provides five scalar values of bias magnetization and an actual geomagnetic field via RS232 serial port. Computer controls and backups the data using custom software adapted to the tasks of magnetic observatories. The records are displayed on the computer monitor (Fig. 6). A more detailed description will be published elsewhere.

The magnetometers were tested at the observatories and Arty and Paratunka for several years. Variant POS-3 measuring module and the only vertical component under the observatory Arti and points secular variation of the earth's magnetic field around town Arti (Sverdlovsk region) are used.

The first POS-4 full vector magnetometer (IdD+F) was tested at the observatory Paratunka for two years. The last set is shown in Fig. 7.

In addition to the state standard in St. Petersburg we used the Observatory Arti to test the metrological parameters by vector magnetometers. The metrological parameters, calibration methods including self-calibration methods will be described in separate publications. Our studies show the first copies of sensitive magnetometers modulo field of about 0.02 nT, and in the component field at 0.1 ÷ 0.3 nT measurement cycles of 1 second (total cycle of 5 seconds with the current data update). Fig. 8 and 9 display the examples of actual records in Arti and Paratunka.

Figure 7. Vector/scalar Overhauser magnetometer POS-4. PET, Paratunka (Petropavlovsk).

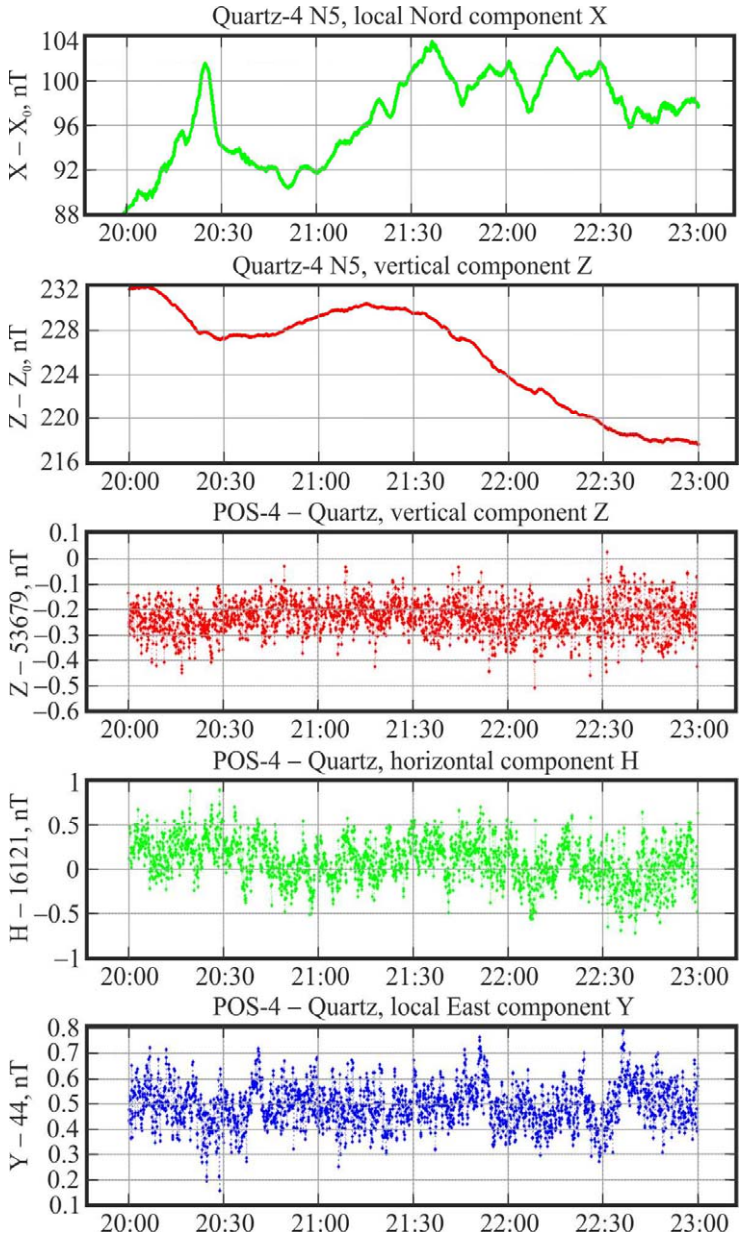

Figure 8. An example of variation Z and X components made is Quartz-4 and Z, H, Y components of POS-4 relative to variometer Quartz-4 (difference to POS-4). RMS ~ 0.1 nT is. 2016:08:11 (UTC). Arti.

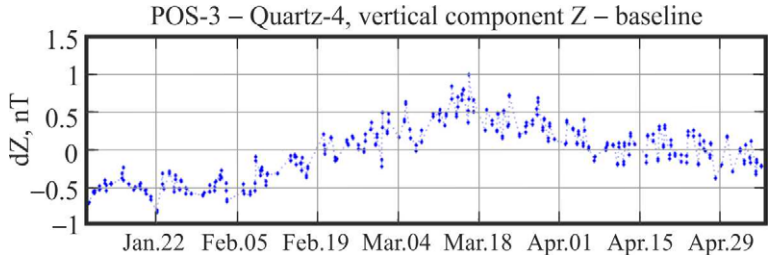

Figure 9. An example of long-term record of the POS-3 (Z) relative to the baseline of the theodolite DIflux magnetometer Theo-010 by taking into account variations of Quartz-4. Stability ~ 2 nT/year is. 2012.

6. Directional drilling support

Modern technologies make it possible to drill wells that practically horizontally enter the oil-bearing layer and may reach reservoirs located several kilometers from the drilling starting point. Such reservoirs may be located under the seabed at a large distance from the shore. Directional drilling requires continuous monitoring of the drill string orientation under the ground. Downhole measurement systems using gyroscopic inclinometers or instruments for measuring magnetic and gravity fields of the Earth are applied for determination of zenith angle and geographic azimuth. Despite certain measuring advantages, gyroscopic inclinometers have a relatively low vibration and impact resistance that results in difficulties with their use in the bottom hole drilling assembly.

Magnetometric technology is more cost effective. Magnetic inclinometers are much more stable and can be used as downhole positioning systems (Fig. 10) to ensure accurate trajectory of directional oil/gas well drilling. However, geomagnetic support of directional drilling in high-latitude regions makes it inevitable to deal with frequent and intense sporadic geomagnetic disturbances associated with the specific geometry of the Earth's magnetic field and solar activity. Geomagnetic perturbations during geomagnetic storms can cause out-of-tolerance high error in downhole magnetometer readings and thus should be filtered. A necessity of establishment of geomagnetic field observations and proper interpretation of the measurement results has led to development of cooperation between oil and gas sector companies, academic geophysical institutions and producers of megnetometric instruments [6, 7].

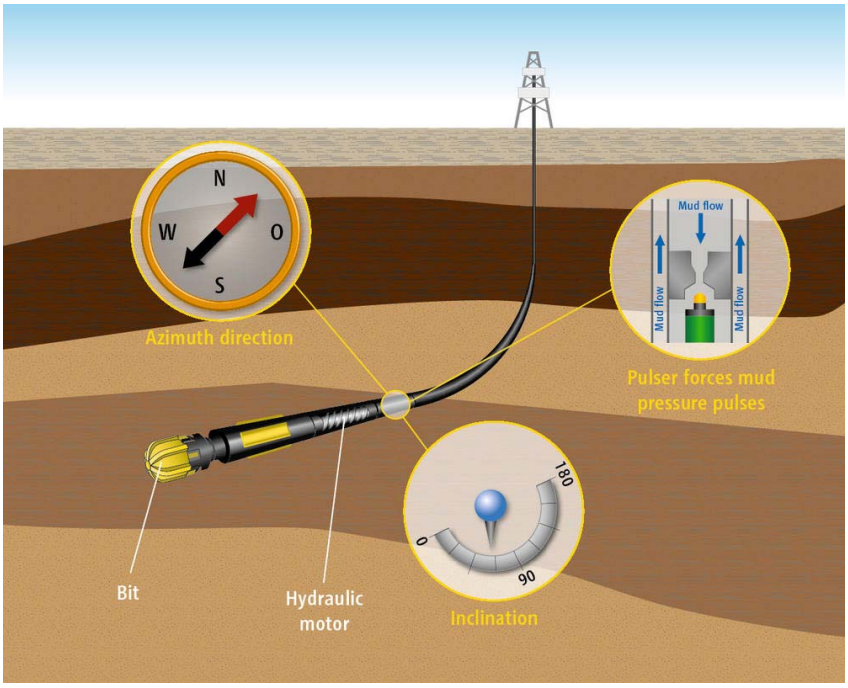

Figure 10. Drilling tool and measuring instruments for controlling specified direction using magnetic declination and inclination down the directional well [8].

Geophysical Center of the Russian Academy of Sciences is involved in geomagnetic field studies, development of scientific foundations and technological capacities in the field of geomagnetic support of directional drilling in the Arctic zone of the Russian Federation, and conduct research on sporadic geomagnetic variations and evolution of the Earth's main magnetic field. Complete range of works include both theoretical (e.g., studies of local geomagnetic effects) and applied (methodological and technological works on the deployment of observatories) tasks [9].

For the timely correction of telemetric magnetic data, streaming from the drilling string, a synchronous independent monitoring of the geomagnetic field is carried out at the Earth's surface using well-instrumented geomagnetic observatories. Their magnetometric equipment should be out of anthropogenic noise that are always present nearby drilling operation sites. As a rule, observatories are installed over a certain distance and mathematical interpolation is applied to data from one or several observatories for correcting Measurement While Drilling (MWD) system readings. Due to the complexity of the operation in the severe northern conditions, the number of observatories in the Arctic is limited [9, 10].

Today the International Real-time Magnetic Observatory Network (INTERMAGNET, [11]) represents the highest quality standard of the full-cycle geomagnetic measurements, needed for providing oil and gas companies with the information on the Earth's magnetic field conditions. Among numerous other requirements to observatory operation [12], INTERMANGET necessitates a minimum essential instrumentation set that includes high-precision vector and scalar magnetometers, as well as absolute magnetometer based on non-magnetic theodolite for regular manual measurements of full magnetic field vector. In the observatory practice, three-axis fluxgate (vector) and proton precession (scalar) magnetometers are commonly used. Usually, these magnetometers have an accuracy of the order of degree 0.1 nT. As a result, geomagnetic observatories provide a complete cycle of very accurate observations, both absolute measurements and measurements of magnetic variations. This distinguishes them from variation stations that measure only magnetic variations [9]. Autonomous magnetic observatories based on the DI+F POS-4 Overhauser vector scalar magnetometer will help develop densely observation network bringing their points of drilling to reduce errors of the gradient variations.

7. Summary

The new IdD+F POS-4 magnetometer is an analog of the famous Canadian dIdD+F magnetometer applied both in observatories, autonomous stations and for directional drilling support of oil and gas wells. The difference is in the absolute component measurement with the vertical orientation. The azimuth angle declination to the geographical north is provided by the telescope on the POS-4 magnetic system and GNSS markup that will be a DI+F absolute vector Overhauser magnetometer.

Acknowledgments

This research was conducted in collaboration with the Geophysical Center of the Russian Academy of Sciences in the framework of the Federal Target Program of the Ministry of Education and Science of the Russian Federation, agreement no. 14.607.21.0058 and ID no. RFMEFI60714X0058. It contributes to the development of the Russian vector magnetometer of the international INTERMAGNET standard.

This work was partially supported by the Russian Science Foundation Grant No. 14-11-00194 and by the subsidy allocated to Ural Federal University for the project part of the state assignment in the sphere of scientific activities TOP 5-100-2020.

References

1. Denisov A., Sapunov V., Rubinstein B. *Meas. Sci. Technol.* **25**, 055103 (2014)
2. Morh P.J., Taylor B.N., Newell D.B. *Reviews of Modern Physics* **84**, 1527 (2012)
3. Sapunov V., Rasson J., Denisov A., Saveliev D., Kiselev S., Denisova O., Khomutov S. *Earth, Planets and Space* **58**, 711 (2006)
4. Lingwood M.D., Han S. *Annual Reports on NMR Spectroscopy* **73**, 83 (2011)
5. Denisov A., Denisova O., Sapunov V., Khomutov S. *Earth, Planets and Space* **58**, 707 (2006)
6. Gvishiani A.D., Lukianova R.Yu., Soloviev A.A. *Gornyi Zhurnal* **10**, 94 (2015) (*in Russian*)
7. Poedjono B., Beck N., Buchanan A., Brink J., Longo J., Finn C.A., Worthington E.W. *Proceedings of the Arctic Technology Conference*, *Houston*, *2012*, **1**, 183 (2012)
8. http://www.dea-group.com/en/technology/drilling/measuring-equipment
9. Gvishiani A., Lukianova R., Soloviev A., Khokhlov A. *Surveys in Geophysics* **35**, 1123 (2014)
10. Gvishiani A.D., Lukianova R.Yu. *Izvestiya, Physics of the Solid Earth* **51**, 157 (2015)
11. http://www.intermagnet.org
12. St-Louis B.J., Sauter E.A., Trigg D.F., Coles R.L., Regimbald D. *INTERMAGNET Technical Reference Manual, Version 4.6, 2012*. INTERMAGNET, Edinburgh (2012)